Tropospheric Duct Anomaly Threat Model for High Integrity and High Accuracy Navigation

Samer Khanafseh and Boris Pervan, *Illinois Institute of Technology*
Axel Von Engeln, *EUMETSAT*

BIOGRAPHY

Dr. Khanafseh is currently a Research Assistant Professor of Mechanical and Aerospace Engineering at IIT. He received his M.S. and PhD degrees in Aerospace Engineering from IIT, in 2003 and 2008, respectively. Dr. Khanafseh has been involved in several aviation applications such as Autonomous Airborne Refueling (AAR) of unmanned air vehicles, autonomous shipboard landing for NUCAS and JPALS programs and Ground Based Augmentation System (GBAS). His research interests are focused on high accuracy and high integrity navigation algorithms for close proximity applications, cycle ambiguity resolution, high integrity applications, fault monitoring and robust estimation techniques. He was the recipient of the 2011 Institute of Navigation Early Achievement Award for his outstanding contributions to the integrity of carrier phase navigation systems.

Dr. Boris Pervan is a Professor of Mechanical and Aerospace Engineering at IIT, where he conducts research on advanced navigation systems. Prior to joining the faculty at IIT, he was a spacecraft mission analyst at Hughes Aircraft Company (now Boeing) and a postdoctoral research associate at Stanford University. Prof. Pervan received his B.S. from the University of Notre Dame, M.S. from the California Institute of Technology, and Ph.D. from Stanford University. He was the recipient of the IIT Sigma Xi Excellence in University Research Award, Ralph Barnett Mechanical and Aerospace Dept. Outstanding Teaching Award, Mechanical and Aerospace Dept. Excellence in Research Award, IIT University Excellence in Teaching Award, IEEE Aerospace and Electronic Systems Society M. Barry Carlton Award, RTCA William E. Jackson Award, Guggenheim Fellowship (Caltech), and the Albert J. Zahm Prize in Aeronautics (Notre Dame). He is an Associate Fellow of the AIAA, a Fellow of the Institute of Navigation (ION), and Editor-in-Chief of the ION Journal Navigation.

Dr. Axel von Engeln is a Radio Occultation/Remote Sensing Scientist at EUMETSAT, Darmstadt, Germany. He received his PhD degree in Physics in 2000 from University of Bermen, Germany. Dr. von Engeln has been working in satellite research for more than 15 years and regularly publishes peer-reviewed first author papers. He first worked with microwave instruments, retrieval algorithms, radiative transfer models, and later focused on the radio occultation technique. Dr. von Engeln has managed several international studies in these fields. He is now working at EUMETSAT on the current radio occultation mission GRAS on Metop-A and -B, is leading the instrument functional chain team for EUMETSAT's next generation radio occultations instrument, and is working with NOAA/NASA on placing a radio occultation receiver on the Jason-CS satellite. Dr. von Engeln is a co-chair of the International Radio Occultation Working Group, the EUMETSAT/ESA Radio Occultation Science Advisory Group, and is the project leader of the SCOPE-CM RO-CLIM.

ABSTRACT

This paper defines a parametric threat model for tropospheric duct anomalies based on fifteen years of tropospheric data. It is shown that tropospheric ducts can produce differential ranging errors on the order of 30 cm. Furthermore, the probability of occurrence of tropospheric duct anomalies (up to 80% in certain locations) is much higher than the integrity and continuity risk requirements used in aviation applications. Because tropospheric ducts are not particularly rare and can cause non-negligible ranging errors, they are potential threats to navigation integrity for high accuracy and integrity applications. The developed threat model, and derived duct error bound, can be used to investigate the impact of tropospheric duct anomalies on the integrity risk and accuracy of the aviation applications.

INTRODUCTION

The troposphere is the lowest part of the earth's atmosphere, extending from earth surface to about 16 km altitude. It is made of electrically neutral gases that are not

uniform in composition, including water vapor and dry gases. Refraction in the troposphere delays the transmission of satellite signals. The tropospheric delay consists of a largely predictable dry component, and of a wet component that varies with location, altitude, season, and weather condition but represents a much smaller fraction of the error. Therefore, the majority of the tropospheric delay can be removed by troposphere modeling. Several models exist that describe the tropospheric delay under nominal conditions. These models include, but are not limited to, Hopfield, Modified Hopfield, and Saastamoinen Models [1].

Under nominal conditions, pressure drops exponentially with height, and temperature decreases with altitude at an approximate rate of 1K/100m (over the first few kilometers above sea level). As a result, the computed refractivity gradient with respect to altitude is approximately -40 /km. For differential satellite ranging implementations, a nominal model of differential tropospheric delays was defined in the context of the Local Area Augmentation System (LAAS). In this model, the refractivity is expressed in terms of reference refractivity N_r, scale height h_0 (typically 7.3 km) and antenna height z as [8]:

$$N = N_r \exp\left(\frac{-z}{h_0}\right) \quad (1)$$

The differential tropospheric delay is then evaluated by integrating N in Equation 1 from the height of the ground station to that of the aircraft, which results in

$$T = 10^{-6} N_r h_0 \left(1 - e^{-\Delta h / h_0}\right) \quad (2)$$

where Δh is the height difference between the aircraft and ship. Equation 2 is used to correct differential measurements under nominal tropospheric condition. In addition, the standard deviation σ_{Trop} of the estimated delay T is derived in reference [8] in terms of the uncertainty in N (with standard deviation σ_N) (Equation 3).

$$\sigma_{Trop} = 10^{-6} \sigma_N h_0 \left(1 - e^{-\Delta h / h_0}\right) \quad (3)$$

Because the correction in Equation 2 is used in the measurement domain, σ_{Trop} can be root-sum-squared (RSS) with the measurement noise standard deviation.

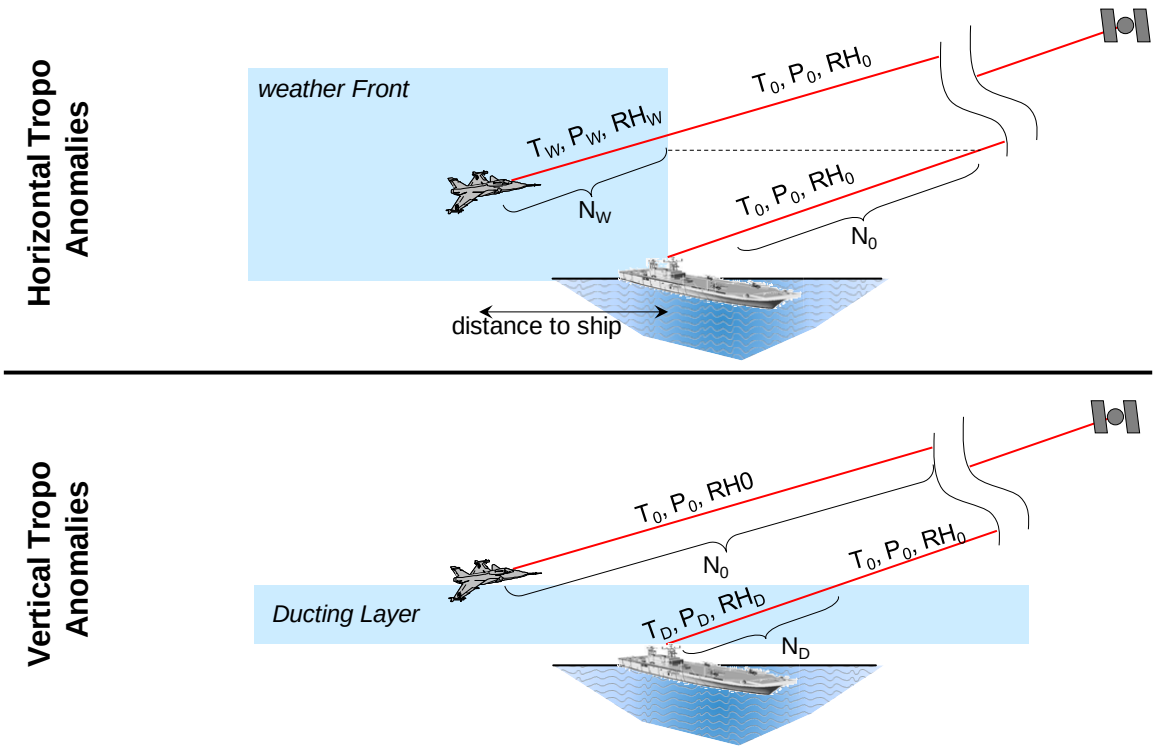

Figure 1: Two Types of Tropospheric Anomalies: Horizontal and Vertical.

In previous work, we investigated the potential of differential carrier phase navigation architectures [2-7] to meet stringent requirements in both accuracy and integrity. We evaluated the impact of residual tropospheric errors, after the nominal tropospheric correction (T in Equation 2) has been removed. Residual errors can be caused by anomalous troposphere causing the delay to differ from the model expressed in Equation 2. Two types of tropospheric anomalies impact high accuracy navigation systems: severe weather fronts and tropospheric ducts (Figure 1). A

weather front is characterized by an abrupt change in refractivity (measured by variations in temperature, pressure, and relative humidity) over short horizontal distances. Published research reports experimental observations of tropospheric delays of up to 40 cm over a 5km distance [9]. Further published work, with application to ground based augmentation systems (GBAS), assumed a 'weather-wall' model to investigate the impact of high stationary fronts on differential ranging measurements (between a user and a local reference station) [10]. This paper focuses on tropospheric duct anomalies.

In the next sections of this paper, vertical tropospheric anomalies or ducts are defined. We describe their causes, and explain their influence on the refractivity index using illustrative examples extracted from a set of experimental data. In a previous work [13], as a preliminary study on tropospheric ducts, duct thickness, altitude and refractivity gradient statistics were quantified and their probability of occurrence was established for six locations. That work illustrates that ducts are potential integrity threats because they can cause large measurement errors relative to differential carrier phase tracking noise, and because they have a high likelihood of occurrence. In contrast to that work, where ducts from only six locations are analyzed, in this work, a new set of 15 years of data is analyzed to compute the zenith error due to tropospheric duct and its likelihood. The computed error is quantified with respect to the probability of occurrence for a worldwide grid of 1 degree resolution. Using this data, a distribution of the zenith duct error is established that can be used to provide a stochastic bound. This stochastic bound can be used to quantify the impact of ducts on differential ranging measurements for aviation applications.

TROPOSPHERIC DUCTS

Under nominal tropospheric conditions, pressure drops exponentially with height, and temperature decreases with altitude at an approximate rate of 1K/100m (over the first few kilometers above sea level), resulting in a refractivity gradient over altitude (in Equation 1) of approximately -40/km. However, this standard behavior does not apply under anomalous atmospheric conditions when tropospheric ducts can be generated. Ducts tend to form when either temperature is increasing, or water vapor concentration is decreasing with height, or both. Mechanisms causing the apparition of ducts include:

1- Temperature inversion: usually, temperature falls with height by about 1K per 100m. In a temperature-inversion layer, the temperature rises with height. For example, on a clear night the ground cools faster causing the air at the surface to be lower in temperature than at higher altitudes.

2- Evaporation ducts: is associated with the sharp drop in moisture above a water surface. It results from the evaporation of water vapor, which causes the water vapor pressure at the sea surface to be saturated while the layer above contains less moisture. The resulting humidity gradient is usually sufficient to maintain a surface duct above the sea surface. This usually occurs over large expanses of water such as the great lakes.

3- Air subsidence: this is a mechanism that can lead to elevated ducts and is associated with high pressure weather systems such as anticyclones. Descending cold air forced downwards by the anticyclone heats up as it is being compressed and becomes warmer than the air near the ground, which leads to an elevated temperature inversion. As the anticyclone evolves, the air at the edges subsides which brings the inversion layer closer to the ground. As a result, the inversion layer becomes lower close to the edge of the anticyclone and higher in the middle.

4- Air advection: this phenomenon occurs when air moves from warm land to cooler sea surface typically in early evenings in summer. This warm air mixes with the cooler moist air over the sea causing the height of the evaporation duct to increase. This also leads to high humidity gradients and a temperature inversion. As a result, a surface duct within the first few 100 meters above the sea is formed. These ducts usually occur over the coastal regions.

Due to the sudden change in temperature and relative humidity caused by ducts, the refractivity will not follow the nominal exponential curve in Equation 1. Example refractivity data from the European Centre for Medium range Weather Forecast (ECMWF) are shown in Figure 2 [11] (Note: we use the improved ERA-Interim re-analysis here, [11] was based on ERA-40). The figure shows examples of refractivity profiles in the presence of ducts at two different locations. It is obvious from the figure that the refractivity gradient when ducts exist (blue curves) is much higher than the nominal case (red curves). In Figure 2-a, the refractivity profile gets back to nominal values right after the initial duct gradient while in Figure 2-b, the convergence between the blue and red curves is quite slow.

We now consider the impact of such ducts on radiofrequency signals. For simplicity, and assuming that the reference station is at zero height, the differential tropospheric delay at any height is the integration of each curve with respect to height. The tropospheric error due to the existence of ducts will therefore be the difference between the two integrals (i.e., the area between the nominal refractivity curve (red) and the duct refractivity curve (blue)). Figure 3 shows the profile of the residual tropospheric error (after removing the nominal

tropospheric correction from the data) corresponding to Figure 2-a. Figure 3 illustrates that the zenith error caused by the duct reaches up to 1 cm. Tropospheric errors affecting satellite signals can be scaled by an obliquity factor to model the fact that low-elevation ranging signals travel across larger sections of the troposphere than high-elevation observations. Taking the obliquity factor into account, an error magnitude of 1 cm in zenith corresponds to a measurement error of 7.7 cm for a 7 degree elevation satellite. Therefore, the duct error affecting carrier phase measurements is much larger than the magnitude of the measurement noise itself (which is in the order of 1 cm).

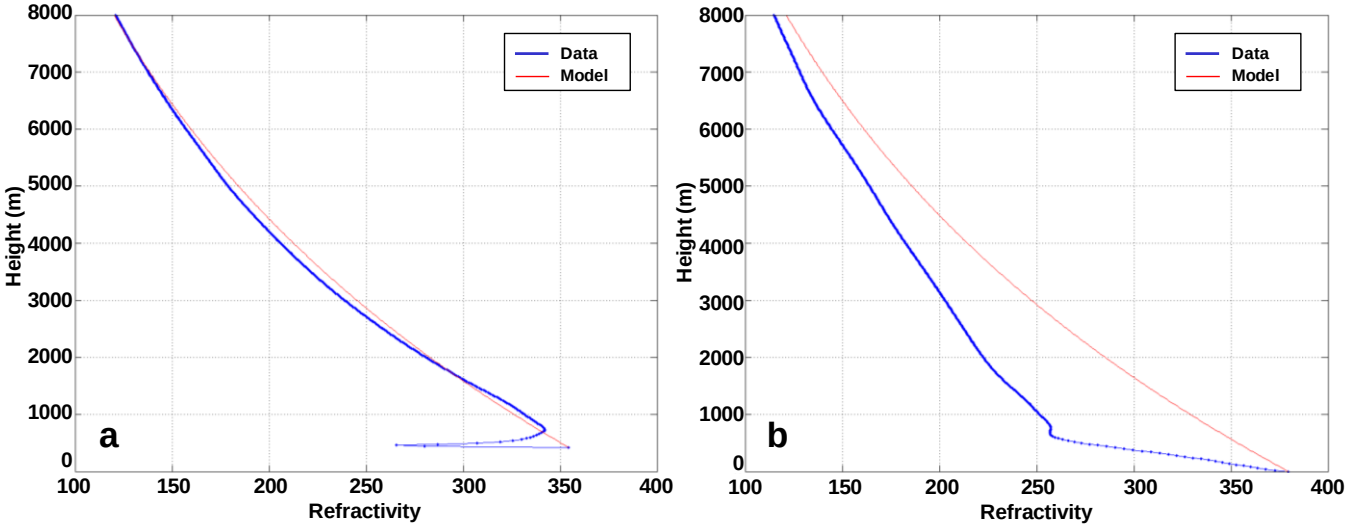

Figure 2: Refractivity Profiles at Two Different Locations (a:25N 97E and b:27N 51E) in the Presence of Ducts. Blue: Refractivity from the ECMWF Model; Red: Nominal Exponential Profile.

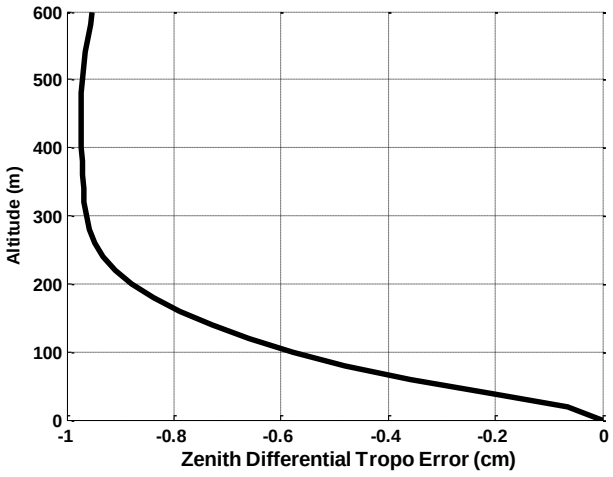

Figure 3: Zenith Differential Tropospheric Error for the First 600 m of the Profile in Figure 2-a.

In addition to the duct error magnitude, another parameter of interest when modeling that type of anomalies is the likelihood of occurrence of ducts. In [11], six years of ECMWF data were analyzed and several duct characteristics were reported. In particular, a global map of duct likelihood of occurrence was established. However, these results included all ducts at all altitudes.

For most aircraft approach applications, and in particular landing application, tight integrity and accuracy requirements are only required close to the runway and at low altitudes (for example, 500 m altitude, corresponds to 10km distance on a 3 degree glide slope). Therefore, if a duct exists at an altitude higher than 500 m, it will be eliminated in the differential process and will not pose any integrity threat. Only ducts that are lower than 500 m will cause modeling errors that might jeopardize integrity. Therefore, a new map of duct likelihood of occurrence is generated in Figure 4 using 15 years of ECMWF data (2000-2014). In this map, only ducts occurring below 500 m are considered. The map illustrates that the likelihood of a duct happening below 500 m is much larger than the integrity risk requirement demanded in most aviation applications. Therefore, the duct's high probability of occurrence combined with its large error magnitude (relative to carrier phase measurement noise) causes it to be a substantial threat for GNSS-based aviation applications.

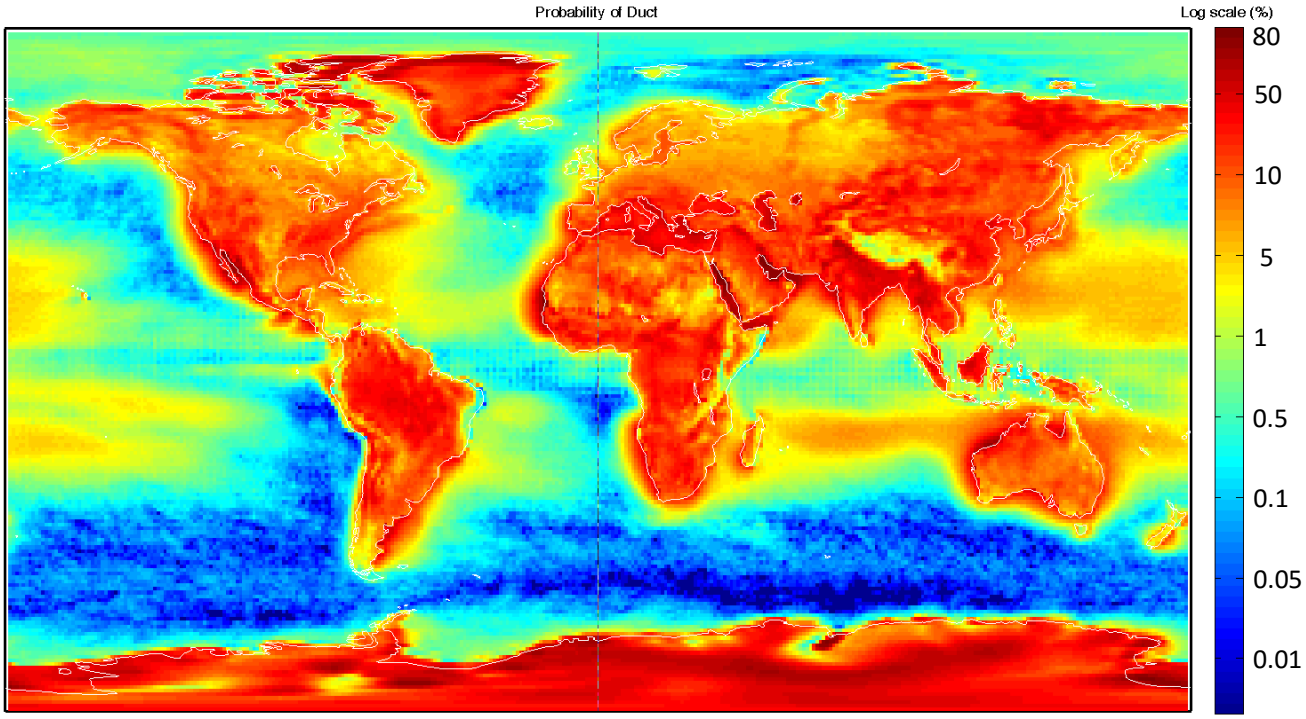

Figure 4: Map of the Ducts' Likelihood of Occurrence

TROPOSPHERIC DUCT THREAT MODEL

The multiple atmospheric parameters influencing a duct and their large range of variation make the definition of a threat model challenging. One approach would be to compute the tropospheric delays caused by each one of the ducts observed in the 15 years of data (analyzed in Figure 3 in the previous section), but this would be computationally extremely demanding. Instead, a simplified duct model that only depends on three parameters is defined. Figure 5 shows the duct 'wedge model', which is defined using the duct altitude (where the duct steep gradient in refractivity starts), duct thickness (the region where the duct gradient is steep, i.e., lower than -160/km), and duct gradient (the average slope of the duct). Using these parameters and the wedge model, the mismodeling residual error due to tropospheric ducts can be analytically determined by computing the area of the triangle (shaded in yellow). It is acknowledged that this model might be optimistic because it assumes that once the duct ends, it instantaneously recovers nominal profile values. This assumption may not be realistic according to Figure 2. However, this preliminary analysis will provide useful information towards establishing the severity of the threat that ducts represent. A more refined model may be considered in the future.

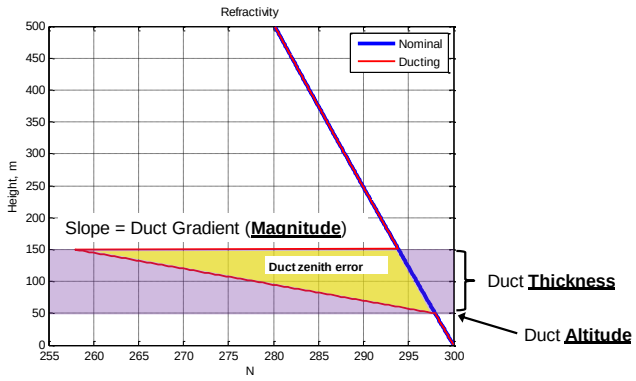

Figure 5: Three-Parameter Wedge Model Used to Account for Ducts

We used the 15 years of ECMWF data to record the three duct-threat parameters (Altitude, thickness and magnitude) and we established a threat model that is based on residual measurement errors directly derived from these parameter combinations. Using these parameters and assuming that the integration is performed at the highest altitude considered here (500 m), the duct error is computed. The tropospheric zenith errors computed based on the wedge model parameter values are then used to generate a map of the worst case duct zenith error observed at each grid point (Figure 6).

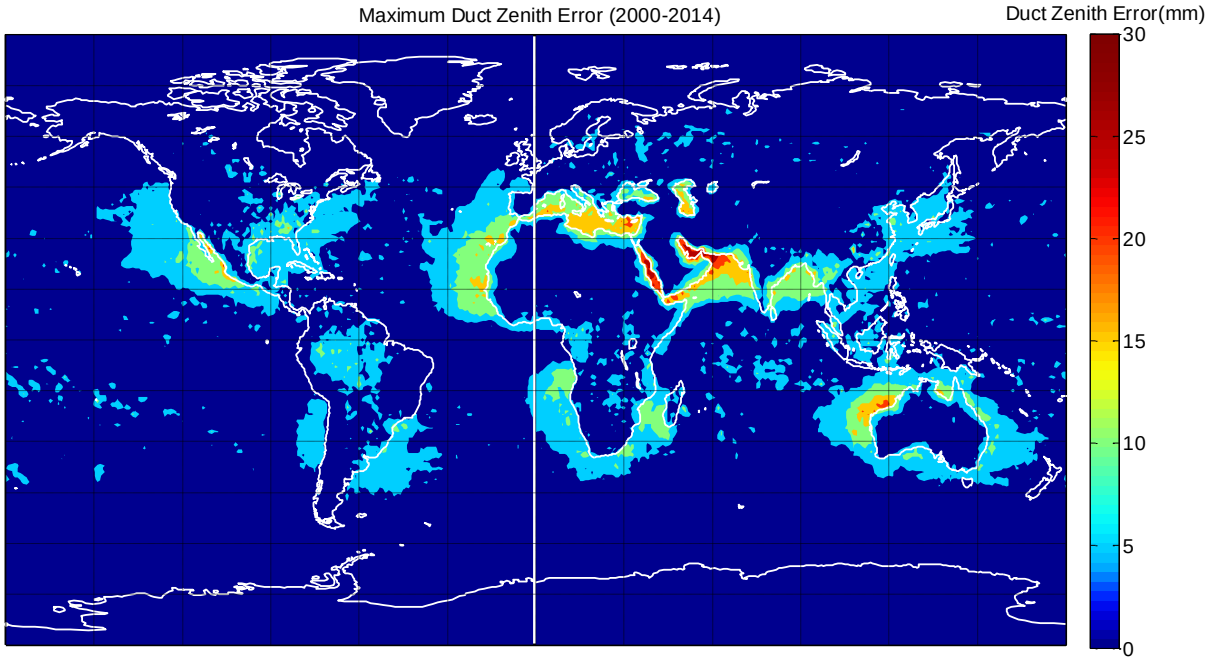

Figure 6: Map of the Ducts' Maximum Zenith Error

Figures 4 and 6 can serve as worst case likelihood and worst case zenith duct error observed at each of these grid points. In order to provide a better stochastic representation of the data, a histogram of the duct error is shown in Figure 7. This histogram shows that for all locations and using the wedge model, the maximum error that was observed at 500m is 30mm in zenith (approximately 23cm for a 7 degree elevation satellite). The histogram also shows that the duct error distribution is non Gaussian and has a non zero mean. However, the histogram also shows that a duct of 30mm error is quite rare and that most of the ducts produce 1mm or less in error. Therefore, the histogram in Figure 7 is converted to a cumulative distribution in Figure 8 assuming the aircrafts are at different altitudes: 33m, 66m, 100m, 200m, 300m, 400m, and 500m. In Figure 8, the error is normalized by the altitude of the aircraft (in the x-axis). The CDF curves were then bounded by a Gaussian CDF with a standard deviation σ of 17mm/km of height difference between the reference station and the user. Although the Gaussian CDF doesn't bound the initial point, the bound is reasonable given that the duct error magnitude is small and can be easily budgeted from the position domain error or alert limit of the application. It was also noticed that when similar plots were generated for land or sea based locations, the same 17mm/km bound was achieved.

For example, for an aircraft in landing approach, the tropospheric standard deviation in Equation 3 can be approximated to

$$\sigma_{Trop} \cong 10^{-6} \Delta h \, \sigma_{\mathrm{N}} \qquad (4)$$

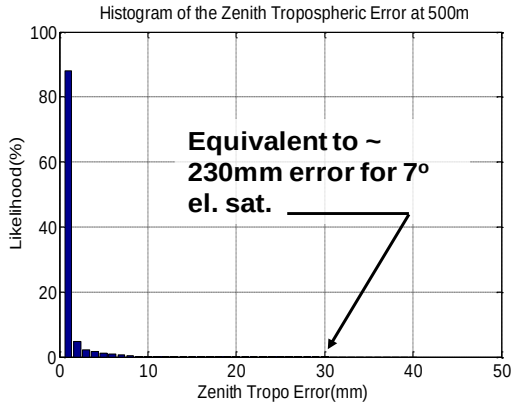

Figure 7: Histogram of the Zenith Tropospheric Error Observed Over 15 Years.

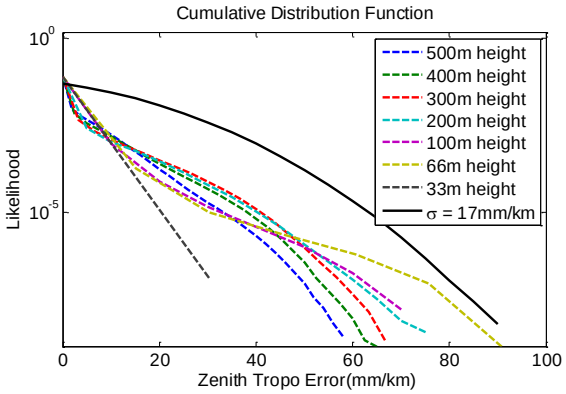

Figure 8: Cumulative Distribution of Tropospheric Duct Errors.

In order to account for tropospheric duct anomalies, and given the bound of 17mm/km in Figure 8, the resultant tropospheric error standard deviation becomes

$$\sigma_{Trop} \cong 10^{-6}\Delta h \sqrt{\sigma_{\mathrm{N}}^2 + 17^2} \quad (4)$$

Noticing that σ_N is typically in the order of 10, it is concluded that the tropospheric duct error should not be ignored and the modified value in Equation 4 is used. Using the tropospheric obliquity factor (mapping function) for each satellite, this error can then be converted to ranging error variance, which then can be added to the other nominal error variance by the user in the estimate measurement noise covariance.

CONCLUSIONS

In this paper, we described tropospheric ducts and illustrated the fact that these anomalies can cause ranging errors of up to 23cm with a likelihood of occurrence that is much larger than the integrity risk of most aviation applications (reaching up to 50% at some locations). A global threat model that describes the duct zenith error and the likelihood for each error magnitude was established. A bound on the effect of the tropospheric duct effect on the ranging measurement error was also derived. It was concluded after accounting for the likelihood of the tropospheric ducts that a standard deviation of 17mm/km of height bounds the tropospheric duct error. The variance of this duct error can then be used to compute the resultant the measurement noise variance in the estimation process.

ACKNOWLEDGMENT

The authors would like to thank Caio Kioshi Miyazaki and Diego Vitoriano da Silva from the Brazilian exchange program IIE for processing the tropospheric duct data. The authors also gratefully acknowledge the Federal Aviation Administration FAA for supporting this research. The opinions presented in this paper are those of the authors and do not necessarily represent those of FAA or any other affiliated agencies.

REFERENCES

[1] P. Misra and P. Enge, Global Positioning System signals, Measurements, and Performance. Lincoln, MA: Ganga-Jamuna Press, 2001.

[2] M. Heo, B. Pervan, S. Pullen, J. Gautier, P. Enge, and D. Gebre-Eziabher, “Robust Airborne Navigation Algorithm for SRGPS,” *Proceedings of IEEE/ION Position, Location, and Navigation Symposium (PLANS '2004)*, Monterey, CA, Apr. 2004.

[3] S. Khanafseh and B. Pervan, “Autonomous Airborne Refueling of Unmanned Air Vehicles Using the Global Positioning System,” *Journal of Aircraft*, Vol. 44, No. 5, Oct. 2007, pp. 1670-1682.

[4] S. Langel, S. Khanafseh, F. C. Chan, B. Pervan, “Cycle Ambiguity Reacquisition in UAV Applications using a Novel GPS/INS Integration Algorithm,” *Proceedings of the 2009 International Technical Meeting of the Institute of Navigation ION-ITM 2009*, Anaheim, CA, Jan. 2009.

[5] S. Dogra, J. Wright, and J. Hansen, “Sea-Based JPALS Relative Navigation Algorithm Development,” *Proceedings of the 18th International Technical Meeting of the Satellite Division of the Institute of Navigation ION GNSS 2005*, Long Beach, CA, Sept. 2005.

[6] G. A. McGraw, “Generalized Divergence-Free Carrier Smoothing with Applications to Dual Frequency Differential GPS,” *NAVIGATION: Journal of Institute of Navigation*, Vol. 56, No. 2, Summer 2009.

[7] Wu, Shuwu, Peck, Stephen R., Fries, Robert M., "Geometry Extra-Redundant Almost Fixed Solutions: A High Integrity Approach for Carrier Phase Ambiguity Resolution for High Accuracy Relative Navigation," *Proceedings of IEEE/ION PLANS 2008*, Monterey, CA, May 2008, pp. 568-582.

[8] McGraw, Gary A., Murphy, Tim, Brenner, Mats, Pullen, Sam, Van Dierendonck, A. J., "Development of the LAAS Accuracy Models," *Proceedings of the 13th International Technical Meeting of the Satellite Division of The Institute of Navigation (ION GPS 2000)*, Salt Lake City, UT, September 2000, pp. 1212-1223.

[9] Huang, Jidong, van Graas, Frank, Cohenour, Curtis, "Characterization of Tropospheric Spatial Decorrelation Errors Over a 5-km Baseline", *NAVIGATION*, Vol. 55, No. 1, Spring 2008, pp. 39-53.

[10] Van *Graas*, F., Zhu, Z., "Tropospheric Delay Threats for the Ground Based Augmentation System," *Proceedings of the 2011 International Technical Meeting of The Institute of Navigation*, San Diego, CA, January 2011, pp. 959-964.

[11] Axel von Engeln, Joao Teixeira, “A Ducting Climatology derived from ECMWF Global Analysis Fields,” *J. Geophys. Res.*, 109 (D18), D18104, doi:10.1029/2003JD004380, 2004.

[12] “Minimum Operational Performance Standards for Global Positioning System/Wide Area Augmentation System Airborne Equipment,” RTCA Document Number DO-229C, Nov. 2001, Appendix B.5.

[13] Khanafseh, S., Joerger, M., Pervan, B., Von Engeln, A., "Accounting for Tropospheric Anomalies in High Integrity and High Accuracy Positioning Applications," *Proceedings of the 24th International Technical Meeting of the Satellite Division of the Institute of Navigation (ION GNSS 2011)*, Portland, OR, September 2011, pp. 513-522.